Running coupling and the Λ parameter from SU(3) lattice simulations

Gunnar S. Bali* and Klaus Schilling

Physics Department, Bergische Universität, Gesamthochschule Wuppertal,
Gauss-strasse 20, 5600 Wuppertal, Germany
(Received 31 August 1992)

We present new results on the static $q\bar{q}$ potential from high-statistics simulations on 32^4 and smaller lattices, using the standard Wilson action at $\beta = 6.0$, 6.4, and 6.8 on the Connection Machine CM-2. Within our statistical errors ($\approx$ 1%) we do not observe any finite-size effects affecting the potential values, on varying the spatial lattice extent from 0.9 fm up to 3.3 fm. We are able to see and quantify the running of the coupling from the Coulomb behavior of the interquark force. From this we extract the ratio $\sqrt{\sigma}/\Lambda_L$. We demonstrate that scaling violations on the string tension can be considerably reduced by introducing effective coupling schemes, which allow for a safe extrapolation of Λ_L to its continuum value. Both methods yield consistent values for Λ: $\Lambda_{\overline{\text{MS}}} = 0.555^{+0.019}_{-0.017} \times \sqrt{\sigma} = 244^{+8}_{-7}$ MeV, where $\overline{\text{MS}}$ denotes the modified minimal subtraction scheme. At the highest-energy scale attainable to us we find $\alpha(5 \text{ GeV}) = 0.150(3)$.

PACS number(s): 11.15.Ha, 12.38.Aw, 12.38.Gc

I. INTRODUCTION

The experimental determination of the running coupling *constant* of QCD has reached a reasonable degree of accuracy [1] after two decades of research effort. This has stimulated considerable attention to compute this quantity from first principles, by use of lattice methods [2–4]. The lattice approach to the problem of matching perturbative and nonperturbative aspects of QCD is notoriously difficult because of the requirement of a high-energy resolution. Nevertheless, computer experiments in pure SU(2) and SU(3) gauge theories have reached a precision that allows to ask rather detailed questions about the static quark-antiquark potential. The size of the available lattices ($48^3 \times 56$, in SU(2) gauge theory [5]) enables one to decrease the lattice spacing a into a regime where one can make contact to predictions of continuum perturbation theory. This has been done for the case of SU(2) by a study of the Coulomb behavior of the interquark force in Ref. [3]. In the case of SU(3), a lattice spacing of $a^{-1} = 3.6$ GeV was achieved so far [6] on a 32^4 lattice at $\beta = 6.4$. This resolution is about the threshold for running coupling effects to become visible.

In this paper we want to present a detailed investigation of the running coupling in SU(3) gauge theory, by further reducing the lattice spacing to $a^{-1} = 6.0$ GeV. Within our analysis of the small-distance regime, we will use a parametrization incorporating lattice effects. Being limited to lattice sizes up to 32^4, we have to make sure that our results are not spoiled by finite-size effects. For this reason we have worked on a variety of lattices, at each value of β.

Once the running coupling has been extracted, we will

be able to compare to perturbative predictions and estimate a value for the corresponding Λ_L parameter. We will see that this value is consistent with Λ_L, as obtained from the string tension (by the use of the two-loop β function [7]), after an extrapolation to $a = 0$. In order to substantiate this result we will improve on scaling violations (as expressed in the strong β dependence of Λ_L) by replacing the bare coupling with suitable "effective" couplings [8–11], measured on the lattice from the average plaquette. In this case we will find nearly asymptotic scaling for $\beta > 6.0$. The extrapolation to the continuum yields an estimate for Λ_L which is consistent within smaller errors with the value obtained from the running coupling.

II. METHODS

A. Sampling

In order to maintain an appropriate stochastic movement of the gauge system through phase space with increasing β, we have combined one Cabibbo-Marinari pseudo-heat-bath-sweep [12] over the three diagonal SU(2) subgroups with 4 (9) successive overrelaxation sweeps [13] for $\beta = 6.4$ (6.8). We reach an acceptance rate of 99.5% for an overrelaxation link update. For the heat bath we use the algorithm proposed by Kennedy and Pendleton [14] which has a high acceptance rate and can thus be efficiently implemented on a single-instruction multiple-data (SIMD) machine. We can afford iterating the algorithm until all link variables are changed. On our local 8K CM-2 we need 9.2 μsec for an overrelaxation link update and 11.5 μsec for a single Cabibbo-Marinari link update. This performance was achieved after rewriting the SU(3) matrix multiply routines in assembler language. Measurements were started after 2000–10 000 thermalization sweeps.

---

*Electronic address: bali@wpts0.physik.uni-wuppertal.de

B. Smoothing operators

In lattice gauge theory physical quantities of interest such as masses, potential values, and matrix elements are related to asymptotic properties of exponentially decreasing correlation functions in Euclidean time, and therefore prone to be drowned in noise. So one is forced to improve operators in order to reach the desired asymptotic behavior for the small-T region. We will shortly describe our particular improvement technique [6].

We start from the relation between Wilson loops $W(R, T)$ and the (ground-state) potential $V(R)$

$$W(R, T) = C(R) \exp \{-TV(R)\}$$
$$+ \text{excited state contributions.} \qquad (1)$$

Our aim is to enhance, for each value of R, the corresponding ground-state overlap $C(R)$. Since the ground-state wave function is expected to be smooth on an ultraviolet scale we concentrate on reducing noise by applying a *local* smoothing procedure on the spatial links: consider a spatial link variable $U_i(n)$, and the sum of the four spatial staples $\Pi_i(n)$ connected to it:

$$\Pi_i(n) = \sum_{\substack{j=\pm 1, \ldots, 3 \\ j \neq i}} U_j(n) U_i(n+\hat{j}) U_j^\dagger(n+\hat{i}). \qquad (2)$$

We apply a gauge-covariant, iterative smoothing algorithm which replaces (in the same checkerboard ordering as the Metropolis update) $U_i(n)$ by $U_i'(n)$ minimizing the local spatial action $S_i(n) = -\mathrm{Re}\,\mathrm{Tr}\{U_i(n)\Pi_i^\dagger(n)\}$, which is qualitatively a measure for the *roughness* of the gauge field. This is very similar to lattice cooling techniques already invented by previous authors [15,16] except that we are *cooling* only within time slices and thus not affecting the transfer matrix. Alternatively, this algorithm may be interpreted as substituting $U_i(n)$ by $\mathcal{P}\,[\Pi_i(n)]$ where $\mathcal{P}$ denotes the projection operator onto the *nearest* SU(3) matrix. In this sense it is a variant of the APE recursive blocking scheme [17] with the coefficient of the straight

link set to *zero*, but with even/odd updating. The latter feature renders the algorithm less memory consuming and seems to improve convergence. Contributions from excited states become increasingly suppressed, as we repeat this procedure. After 30 (45) such smoothing steps at $\beta = 6.4$ (6.8) we reach values for the overlap C (R) of 95 (80)% for small (large) spatial separations R.

C. Extraction of potential values

For the extraction of the potential from the Wilson loop data we proceed essentially as described in Ref. [6], with a slight modification that helps to carry out a straightforward error analysis. Instead of fitting the Wilson loops to the dependence

$$W_{\mathbf{R}}(T; C(\mathbf{R}), V(\mathbf{R})) := C(\mathbf{R}) \exp \{-V(\mathbf{R})T\} \qquad (3)$$

for $T \geq T_{\min}$ with some reasonable cutoff $T_{\min}$ we take the *local mass*

$$V_{T_{\min}}(\mathbf{R}) = \ln \left\{ \frac{W(\mathbf{R}, T_{\min})}{W(\mathbf{R}, T_{\min} + 1)} \right\} \qquad (4)$$

as an estimator for the potential $V(\mathbf{R})$. By using this explicit formula for the calculation of $V(\mathbf{R})$ we are able to propagate the covariance matrix between Wilson loops to a covariance matrix for the potential values. This allows one to separate the determination of potential parameters from the measurement of the potential itself, helping to decrease the degrees of freedom and promoting stability within the fitting procedure. Note that the value of $V(\mathbf{R}) = V_{T_{\min}}(\mathbf{R})$ does not differ appreciably from the result of a fit to Eq. (3) because the latter is anyhow dominated by the lowest two T data due to their small relative errors.

The optimization of the overlap $C(\mathbf{R})$ proceeds as described in Ref. [6]: The parameters $C(\mathbf{R})$ and $V(\mathbf{R})$ are fitted for different $T_{\min}$ to the Wilson loop data separately for each smoothing step (and $\mathbf{R}$) according to Eq. (3) by minimizing

$$\chi_{\mathbf{R}}^2(C(\mathbf{R}), V(\mathbf{R})) = \sum_{T_1, T_2} [W(\mathbf{R}, T_1) - W_{\mathbf{R}}(T_1; C(\mathbf{R}), V(\mathbf{R}))] \left(C^{\mathbf{RR}}\right)^{-1}_{T_1 T_2} [W(\mathbf{R}, T_2) - W_{\mathbf{R}}(T_2; C(\mathbf{R}), V(\mathbf{R}))]. \qquad (5)$$

$C^{\mathbf{R}_1 \mathbf{R}_2}_{T_1 T_2}$ denotes the covariance matrix which is estimated to be

$$C^{\mathbf{R}_1 \mathbf{R}_2}_{T_1 T_2} = \frac{1}{N(N-1)} \sum_{i=1}^{N} [W_i(\mathbf{R}_1, T_1) - W(\mathbf{R}_1, T_1)][W_i(\mathbf{R}_2, T_2) - W(\mathbf{R}_2, T_2)]. \qquad (6)$$

We have divided the time series of Wilson loops into N successive subsets of given length n. $W_i(\mathbf{R}, T)$ stands for the average of the respective Wilson loop over the ith subset. n should be chosen such that $\tau \ll n \ll N$, in order to cope with the autocorrelation time τ. Afterward for each value of $\mathbf{R}$ the smoothing step with highest ground-state overlap $C(\mathbf{R})$ is selected from the fits with reasonable χ^2.

In a second step stability of local masses $V_T(\mathbf{R})$ [Eq. (4)] against variation of T is checked, and $T_{\min}(\mathbf{R})$ is determined as the T value (plus *one*) from which onward stability within errors is observed. For large R values we find $T_{\min} = 4$. For simplicity we chose the same value for small R.

As promised, we are now able to propagate the covariance matrix between different Wilson loops $C^{\mathbf{R}_1 \mathbf{R}_2}_{T_1 T_2}$ to a

TABLE I. The simulated lattices. Physical units correspond to the choice $\sqrt{\sigma} = 440$ MeV for the string tension. Errors ignore the experimental uncertainty within the value of the string tension.

$V = L_S^3 \times L_T$	$\beta = 6.0$		$\beta = 6.4$			$\beta = 6.8$	
	32^4	$16^3 \times 32$	$24^3 \times 32$	$32^3 \times 16$	32^4	$16^3 \times 64$	32^4
a/fm	0.101 (2)		0.0544 (5)			0.0327 (5)	
a^{-1}/GeV	1.94 (5)		3.62 (4)			6.02 (10)	
aL_S/fm	3.25 (8)	0.87 (1)	1.31 (1)		1.74 (2)	0.52 (1)	1.05 (2)
$(aL_T)^-$ MeV	61 (1)	113 (1)		226 (2)	113 (1)	94 (2)	188 (3)
Total no. of sweeps	6100	11 900	22 000	10 000	8900	20 400	15 900
Thermalization phase	1000	2000	2100	2100	2500	10000	5000
No. of measurements	102	100	200	80	65	105	110

covariance matrix between the potential values $C_V^{\mathbf{R_1 R_2}}$, by using the quadratic approximation[1]

$$
\begin{aligned}
C_V^{\mathbf{R_1 R_2}} &= \sum_{T_1 T_2} \frac{\partial V(\mathbf{R_1})}{\partial W(\mathbf{R_1}, T_1)} C_{T_1 T_2}^{\mathbf{R_1 R_2}} \frac{\partial V(\mathbf{R_2})}{\partial W(\mathbf{R_2}, T_2)} \\
&= \frac{C_{T(\mathbf{R_1}), T(\mathbf{R_2})}^{\mathbf{R_1 R_2}}}{W(\mathbf{R_1}, T(\mathbf{R_1})) W(\mathbf{R_2}, T(\mathbf{R_2}))} + \frac{C_{T(\mathbf{R_1})+1, T(\mathbf{R_2})+1}^{\mathbf{R_1 R_2}}}{W(\mathbf{R_1}, T(\mathbf{R_1}) + 1) W(\mathbf{R_2}, T(\mathbf{R_2}) + 1)} \\
&\quad - \frac{C_{T(\mathbf{R_1})+1, T(\mathbf{R_2})}^{\mathbf{R_1 R_2}}}{W(\mathbf{R_1}, T(\mathbf{R_1}) + 1) W(\mathbf{R_2}, T(\mathbf{R_2}))} + \frac{C_{T(\mathbf{R_1}), T(\mathbf{R_2})+1}^{\mathbf{R_1 R_2}}}{W(\mathbf{R_1}, T(\mathbf{R_1})) W(\mathbf{R_2}, T(\mathbf{R_2}) + 1)}
\end{aligned}
\tag{7}
$$

where $T(\mathbf{R})$ is used as an abbreviation for $T_{\min}(\mathbf{R})$. With this covariance matrix we are able to fit the potential data to various parametrizations, incorporating all possible correlations between different operators measured on individual configurations as well as correlation effects within the Monte Carlo time series of configurations.

D. Measurements

The lattice parameters used for the simulations[2] are collected in Table I which includes quotations of 32^4 lattices at $\beta = 6.0$ and $\beta = 6.4$, as well as a $24^3 \times 32$ lattice at $\beta = 6.4$ that have been simulated recently [6], and are reanalyzed in the present investigation. The spatial extent of the lattices at $\beta = 6.4$ ranges from $aL_S = 0.87$ fm to 1.74 fm. At $\beta = 6.8$ lattice volumes of $(0.52$ fm$)^3$ and $(1.05$ fm$)^3$ have been realized. The resolution a^{-1} is varied from 1.9 GeV to 6.0 GeV.

Smoothened on- and off-axis Wilson loops were measured every 100 sweeps (every 50 sweeps for $\beta = 6.0$). Up to $N_{\max} = 30$ (45) smoothing steps were performed at $\beta = 6.0, 6.4$ (6.8). The following

spatial separations were realized: $\mathbf{R} = M\mathbf{e}_i$ with $\mathbf{e}_i = (1,0,0), (1,1,0), (2,1,0), (1,1,1), (2,1,1), (2,2,1)$. M was increased up to $L_S/2$ for $i = 1, 2, 4$, and up to $L_S/4$ for the remaining directions. Altogether this yields 72 different separations $\mathbf{R}$ on the $32^3 \times L_T$ lattices. The time separations $T = 1, 2, \ldots, 10$ were used. Thus the total number of operators measured on one configuration ($V = 32^3 \times L_T$) is $72 \times 10 \times N_{\max}$.

The potential values at $\beta = 6.0$ and $\beta = 6.4$ have been listed in our previous publication [6]. For the convenience of the reader we collect the corresponding values for $\beta = 6.8$ in the Appendix.

III. RESULTS

A. $q\bar{q}$ potential

We connect our investigation to the recent SU(2) analysis by Michael [3], and start from his ansatz

$$
V(\mathbf{R}) = V_0 + KR - e\left(\frac{1-l}{R} + l\,4\pi G_L(\mathbf{R})\right) + \frac{f}{R^2}.
\tag{8}
$$

The lattice propagator for the one-gluon exchange [20],

$$
G_L(\mathbf{R}) = \int_{-\pi}^{\pi} \frac{d^3 k}{(2\pi)^3} \frac{\cos(\mathbf{k} \cdot \mathbf{R})}{4 \sum_i \sin^2(k_i/2)},
\tag{9}
$$

has been calculated numerically. The parameter l is expected to be in the range $0 \leq l \leq 1$ and controls the violation of rotational symmetry on the lattice (within this ansatz). The term f/R^2 mocks deviations from a pure Coulomb behavior and is expected to be positive to the extent that asymptotic freedom becomes visible in the effective Coulomb term $-(e - f/R)/R$.

---

[1]In order to check the validity of this approximation, we have moreover carried out a bootstrap analysis [18] of our data on the 32^4 lattices. (This method is also shortly described in the Appendix of Ref. [19].) The resulting errors (and biased values) are almost identical with the results of our approximation, but the bootstrap method alone does not deliver reliable χ^2 values (incorporating the correlation effects).

[2]Note that we have adapted the physical scales from $\sqrt{\sigma} = 420$ MeV to $\sqrt{\sigma} = 440$ MeV.

TABLE II. Fit results. Since the parameter values on the largest lattices are most precise, we refrain from citing results gained on smaller volumes as long as they are compatible with the stated numbers. For the $16^3 \times 64$ lattice at $\beta = 6.8$ this is not the case. Therefore we have listed both the standard fit result and the parameter values with the string tension constrained to its 32^4 value.

	$\beta = 6.0$	$\beta = 6.4$	$\beta = 6.8$		
Vol.	32^4	32^4	32^4	$16^3 \times 64$	
K	0.0513 (25)	0.014 75 (29)	0.005 33 (18)	0.005 45(27)	0.005 33
e	0.275 (28)	0.315 (15)	0.311 (10)	0.269 (22)	0.274 (18)
V_0	0.636 (10)	0.6013 (37)	0.5485 (24)	0.5412 (37)	0.5426 (34)
l	0.64 (12)	0.564 (55)	0.558 (35)	0.725 (87)	0.710 (120)
f	0.041 (58)	0.075 (18)	0.094 (13)	0.037 (26)	0.043 (25)
$R_{\min}$	2	$\sqrt{3}$	$\sqrt{3}$	$\sqrt{3}$	$\sqrt{3}$
$\frac{\chi^2}{N_{DF}}$	0.816	0.953	0.937	0.989	0.754

A test of the ansatz Eq. (8) implies that the "corrected" data $V(R) = V(\mathbf{R}) + \delta V(\mathbf{R})$ with

$$\delta V(\mathbf{R}) = el[4\pi G_L(\mathbf{R}) - 1/R] \qquad (10)$$

are independent of the direction of $\mathbf{R}$. The global situation is depicted for the 32^4 lattice at $\beta = 6.4$ in Fig. 1 where the corrected data points are plotted together with the interpolating fit $V(R) = V_0 + KR - e/R + f/R^2$, with fit parameters V_0, K, e, and f as given in Table II. Our potential fits yield $\chi^2/N_{DF} < 1$ as long as the first two[3]

data points are excluded. The stability of the string tension result with respect to cuts in R is displayed in Fig. 2 (for $\beta = 6.4$ and 6.8).

For $\beta \geq 6.4$ the Coulomb coefficients e are definitely different from the value $\pi/12 \approx 0.262$ predicted by the string vibrating picture [21] for large $q\bar{q}$ separations. The self-energy contribution V_0 follows the leading-order expectation $V_0 \propto 1/\beta$. We emphasize that for all β values the parameter f is established to be positive as expected. In fact, this parameter tends to increase with β, weakening the Coulomb coupling for small distances.

A more sensitive representation of the scatter of the data points around the interpolating fit curve (obtained on the 32^4 lattice) is shown in Fig. 3 (for $\beta = 6.4$). Note
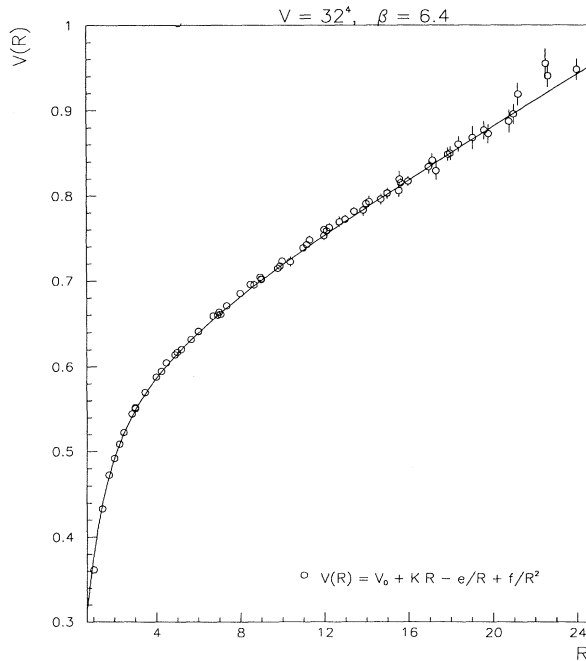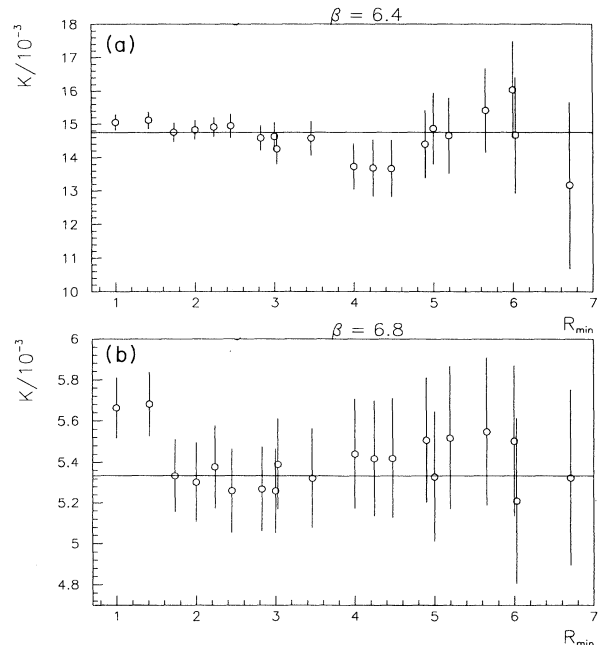
FIG. 1. The $q\bar{q}$ potential at $\beta = 6.4$ (in lattice units). The data points have been corrected for the lattice Coulomb propagator [Eq. (8)]. The fit parameters are contained in Table II.

[3]Three for $\beta = 6.0$.

FIG. 2. The values for the string tension K at (a) $\beta = 6.4$ and (b) $\beta = 6.8$ are plotted against the smallest R separation included for the corresponding fit in order to visualize stability. The first two values (in each figure) have nonreliable error bars since $\chi^2 > N_{DF}$.
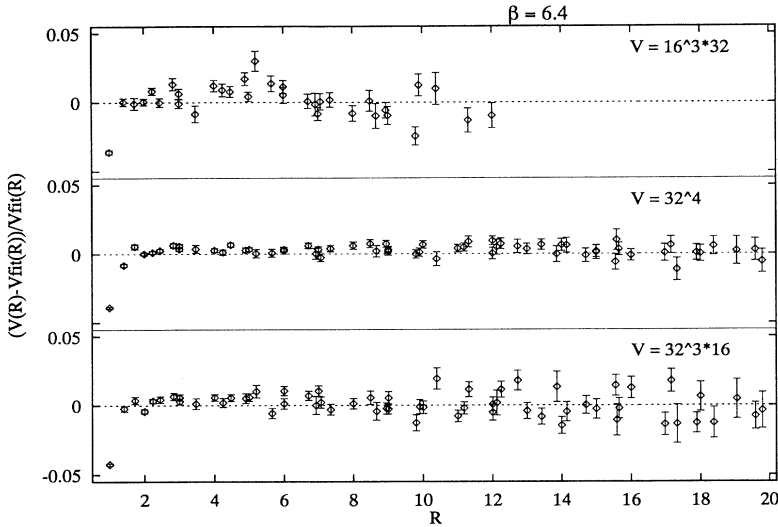
FIG. 3. The relative deviation between the potential values and the corresponding fit curve (taken from a fit to the 32^4 data) is shown for the $16^3 \times 32$, 32^4, and $32^3 \times 16$ lattices for $\beta = 6.4$, respectively.

that the deviations are within a 1% band for the largest volume, once the first two data points are excluded. Decreasing the lattice spatially or in the time direction by a factor of 2 leaves the data points compatible with the interpolating curve, i.e., the finite-size effects (FSE's) are below our statistical accuracy. Nevertheless it pays to work on a 32^4 lattice since the larger possible $q\bar{q}$ separations increase the lever arm needed to fix the long-distance part of the potential.

At $\beta = 6.8$ we find indications of FSE's by comparing results from the small lattice and the 32^4 lattice. As the string tension appears not to suffer from these effects, we have fixed its value to that measured on the larger lattice in order to study FSE's on the remaining parameters more directly. The largest FSE occurs for the lattice correction parameter l. This may be due to the low-momentum cutoff that starts to become visible on the scale of a few lattice spacings. By choosing the form of the one-gluon exchange [Eq. (9)] we have neglected this cutoff in the integral bounds.

We concentrate our interest here on short-distance physics where the linear term is not yet dominating the potential. In the case of $\beta = 6.4$ the latter happens at $R \approx 5$. From Fig. 3 we conclude that reliable results can be extracted from a lattice as small as 16^3 for this β value. In physical units this corresponds to a 27^3 lattice at $\beta = 6.8$. So a volume of 32^3 (or even smaller) appears to be sufficiently large for our purpose.

A synopsis of data for $\beta = 6.0, 6.4$, and 6.8, in physical units, is displayed in Fig. 4 with logarithmic ordinate ranging from 0.03 fm up to 1.9 fm. The three data sets collapse to a universal potential. The two curves correspond to a linear-plus-Coulomb parametrization, with the string tension $\sigma = Ka^{-2}=(440 \text{ MeV})^2$, and the strength of the Coulomb term determined by our fit to the $\beta = 6.4$ data ($e = 0.315$, solid curve), and fixed to the Lüscher value ($e = \pi/12$, dashed curve), respectively. The plot demonstrates the incompatibility of the data points with a pure Coulomb behavior for short distances, and the necessity of additional terms such as f/R^2.

B. Running coupling

Our lattice analysis for the running coupling $\alpha_{q\bar{q}}(R)$ closely follows the procedure suggested in Ref. [3]. We start from the symmetric discretization in terms of the force F:

$$\alpha_{q\bar{q}}(R) = -\tfrac{3}{4}R_1 R_2 F(R)$$
$$= \frac{3}{4}R_1 R_2 \frac{V(R_1) - V(R_2)}{R_1 - R_2}, \qquad (11)$$
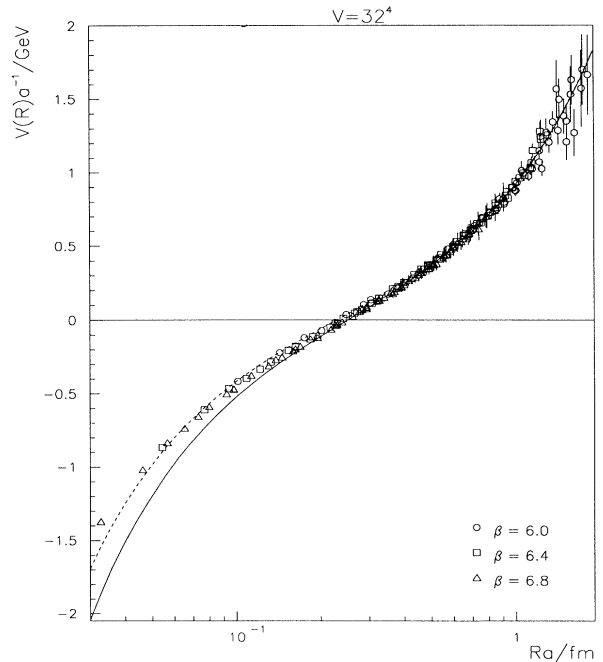

FIG. 4. All "corrected" potential data for the 32^4 lattices at $\beta = 6.0, 6.4$, and 6.8 are scaled to a universal curve by subtracting V_0, and measuring energies and distances in physical units, exploiting the relation $\sqrt{\sigma} = \sqrt{K}a^{-1} = 440$ MeV. The dashed curve corresponds to $V(R) = KR - \frac{\pi}{12R}$, the solid line represents $V(R) = KR - 0.315/R$.

with $R = (R_1 + R_2)/2$. We take the corrected potential $V(R_i) = V(\mathbf{R}_i) + \delta V(\mathbf{R}_i)$ with $\delta V(\mathbf{R}_i)$ as given in Eq. (10). Unlike Ref. [3], however, we use all possible combinations $\mathbf{R}_1, \mathbf{R}_2$ with $|\mathbf{R}_1 - \mathbf{R}_2| < 1.5$.

The resulting data points are contained in Fig. 5(a). In order to exhibit both the global behavior, and the perturbative region ($R \to 0$) we decided to use a logarithmic ordinate (in units of $\sigma^{-1/2}$). The latter region is expanded in the inset. We omitted all values with errors $\Delta \alpha_{q\bar{q}}(R) > \alpha_{q\bar{q}}(R)/3$ in order not to clutter the graph. In addition to the statistical error of the force $F(R)$ we allow for a systematic error

$$\Delta F_{\text{syst}}(R) = \left[\left(\frac{\Delta l}{l} \right)^2 + \left(\frac{\Delta e}{e} \right)^2 \right]^{1/2} |\delta F(R)| \quad (12)$$

with $\delta F(R) = \frac{\delta V(\mathbf{R}_1) - \delta V(\mathbf{R}_2)}{R_1 - R_2}$. ΔF_{syst} is typically of the order of 10% of the lattice correction $\delta F(R)$.

Now we can proceed to analyze our $\alpha_{q\bar{q}}$ data in terms of the continuum large-momentum expectation for the running coupling:

$$\alpha_{q\bar{q}}(R) = \frac{1}{4\pi} [b_0 \ln (Ra\Lambda_R)^{-2} + b_1/b_0 \ln \ln (Ra\Lambda_R)^{-2}]^{-1}, \quad (13)$$

with

$$b_0 = \frac{11}{3} \frac{N_C}{16\pi^2}, \quad b_1 = \frac{34}{3} \left(\frac{N_C}{16\pi^2} \right)^2, \quad (14)$$

being the first two coefficients of the weak-coupling

expansion of the SU(N_C) Callan-Symanzik β function [Eq. (25) below]. In order to extract Λ_R we base our fits exclusively on data points at $\beta = 6.8$ with $R_1, R_2 \geq \sqrt{3}$ on the right-hand side of Eq. (11). This is done in order to avoid the danger of "pollution" from discretization errors.

We now ask the question, within which R region our data are compatible, if at all, with the asymptotic behavior of Eq. (13). We find that as long as $R\sqrt{K} < 0.173$ our fits yield results with reasonable χ^2/N_{DF}. This upper limit in R corresponds to 2.5 GeV. Fitting the $\beta = 6.8$ data over this region we obtain

$$\Lambda_R = (0.562 \pm 0.020 \pm 0.010)\sqrt{\sigma}$$
$$\approx (247 \pm 10) \text{ MeV}. \quad (15)$$

The first error stems from the fit just described, while the second relates to the statistical uncertainty of the string tension within our lattice analysis. The corresponding fit curve with error bands is plotted in Fig. 5. As the data appear to osculate the asymptotic curve one finds a systematic dependence on the R cut: Λ_R tends to be larger if more (low-energy) data points are included and vice versa. In this sense one might consider our value as an upper limit.

Exploiting the relation $\Lambda_R = 30.19\Lambda_L$ [22] we get

$$\Lambda_L^\alpha = (18.6 \pm 0.7 \pm 0.3) \times 10^{-3}\sqrt{\sigma}$$
$$\approx (8.19 \pm 0.33) \text{ MeV}. \quad (16)$$
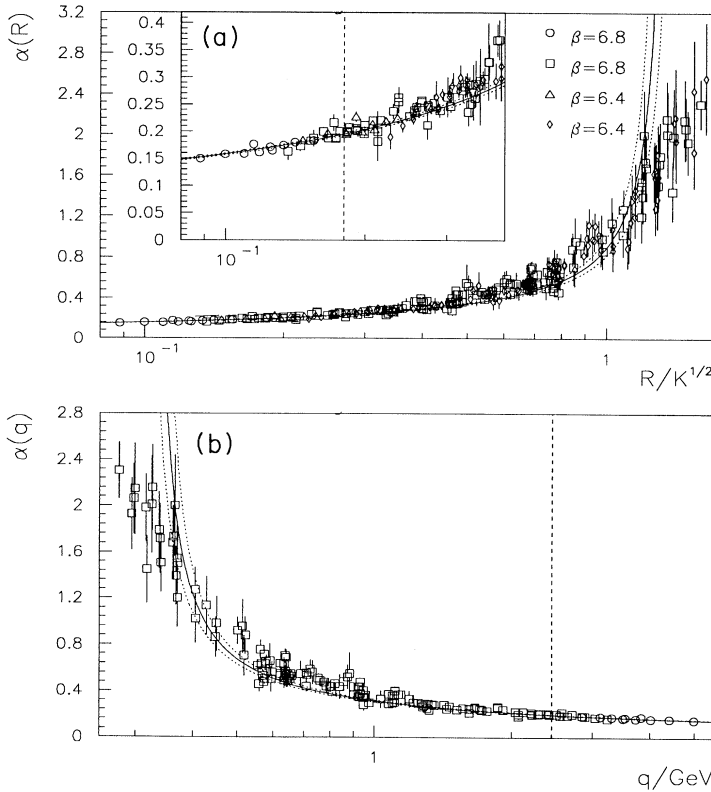
This corresponds to the ratio

FIG. 5. The running coupling $\alpha_{q\bar{q}}$ is plotted versus (a) the $q\bar{q}$ separation and (b) the corresponding energy scale. The circles and triangles might be "polluted" by lattice artifacts (criterion from Sec. III B). The fit curves correspond to the two-loop formula equation (13) with the value $\Lambda_R = 0.562(20)\sqrt{K} = 247(9)$ MeV. If we exclude data points on the large-R (small-q) side of the dashed vertical lines we obtain $\chi^2/N_{\text{DF}} < 1$ values.

$$\frac{\sqrt{\sigma}}{\Lambda_L^\alpha} = 53.7 \pm 2.1. \tag{17}$$

In Fig. 5(b) we have plotted α versus the energy. At the largest realized energy scale we find $\alpha_{q\bar{q}}(5\ \text{GeV}) \approx 0.150(3)$.

Returning to the global structure of the data displayed in Fig. 5 we make three observations. (1) The small-R contributions (circles and triangles) follow very neatly the asymptotic perturbative prediction equation (13), indicating very little discretization effects. (2) Over the whole R range the data sets for $\beta = 6.4$ and $\beta = 6.8$ coincide very nicely, giving evidence for scaling. (3) The deviations of the data from the asymptotic behavior remain fairly small up to $q \approx 1$ GeV or $\alpha_{q\bar{q}} \approx 0.4$.

We conclude that lattice simulations can indeed make contact to the perturbative regime. Moreover, it is very satisfying to observe that the two-loop formula describes the lattice data down to a scale as small as 1 GeV— at least in the quenched approximation of QCD. One would expect that the situation in full QCD is fairly similar, concerning this property. In the infrared regime ($q < \sqrt{\sigma}$) the differences between both theories will be considerable. Because of the linear-confining potential our expectation for the pure gauge sector is $\alpha_{q\bar{q}}(q) \propto 1/q^2$. This has to be confronted with the expression $\alpha_{q\bar{q}}(q) \propto e^{-\mu/q}/q^2$ for QCD with fermionic degrees of freedom where μ stands for the screening mass.

C. Scaling

Normally one speaks of asymptotic scaling when the ratio $\sqrt{\sigma}/\Lambda_L$ remains constant on varying β where

$$\Lambda_L = \frac{1}{a}\exp\left(-\frac{1}{2b_0 g^2}\right)(b_0 g^2)^{-\frac{b_1}{2b_0^2}} \tag{18}$$

(with $g^2 = 2N_C/\beta$) denotes the integrated two-loop β function [Eq. (25) below]. In Table III we have compiled our new results on the string tension together with previous results from Refs. [6, 23]. As can be seen we are still far away from the asymptotic scaling region up to $\beta = 6.8$.

We attempt to extrapolate Λ_L^{-1} to the continuum limit by the use of a parametrization that takes into account the leading-order expectation for scaling violations $O(1/\ln a)$:

$$\Lambda_L^{-1}(a) = \Lambda_L^{-1}(0) + \frac{C}{\sqrt{\sigma}\ln(Da\sqrt{\sigma})}. \tag{19}$$

We find the data compatible with this logarithmic behavior, with $D \approx 1\text{-}2$, and $C \approx 20\text{-}80$. The fit parameters are not particularly stable with respect to a variation of the number of data points. The bandwith of extrapolations to the continuum limit is illustrated in Fig. 6(a) where we have plotted the extreme cases of a fit to our four low-a data points, and all seven data points (open circles). If we average the values obtained from these fits, and take the upmost and the lowest possible numbers as error bandwidth, we estimate the asymptotic value to be $\sqrt{\sigma}\Lambda_L(0)^{-1} = 54^{+18}_{-15}$ (solid circle). We would like to mention that a naive linear extrapolation to the continuum limit yields the value $\sqrt{\sigma}\Lambda_L(0)^{-1} = 63.6$ (2.4) with (obviously) underestimated error. We take this as a warning for purely phenomenological continuum extrapolations.

In view of the uncertainty of the above number it would be highly desirable to improve the situation by developing a scheme within which the a dependence of $\Lambda_L(a)$ is reduced. Parisi suggested many years ago a more "natural" expansion parameter g_E [8], based on a mean field argument. His scheme was elaborated in Refs. [9–11]. It works as follows. Let c_n be the coefficients of the weak-coupling expansion of the average plaquette:

$$\langle S_\square \rangle = \frac{1}{6V}\sum_\square \left(1 - \frac{1}{N_C}\text{Re Tr}\,U_\square\right)$$

$$= \sum_{n=1}^{\infty} c_n g^{2n}. \tag{20}$$

The idea, now, is to introduce an effective coupling in terms of the Monte Carlo generated average plaquette,

$$g_E^2 = \frac{\langle S_\square \rangle}{c_1}$$

$$= g^2 + \frac{c_2}{c_1}g^4 + \frac{c_3}{c_1}g^6 + O(g^8), \tag{21}$$

TABLE III. The lattice spacing a and cutoff parameters Λ_L, calculated from the two-loop-expansion equation (18) in units of the string tension σ. Λ_L is obtained by inserting the bare lattice coupling. For $\Lambda_L^{(1,2)}$ the $\beta_E^{(1,2)}$ effective couplings were used. A naive linear extrapolation to $a = 0$ leads to the results displayed in the second to last row. Logarithmic extrapolations yield the values in the last row.

β	$a\sqrt{\sigma}$	$\sqrt{\sigma}/\Lambda_L$	$\sqrt{\sigma}/\Lambda_L^{(1)}$	$\sqrt{\sigma}/\Lambda_L^{(2)}$
5.7	0.4099 (24)	124.7 (0.7)	63.3 (0.4)	55.7 (0.3)
5.8	0.3302 (30)	112.4 (1.0)	63.0 (0.6)	55.6 (0.5)
5.9	0.2702 (37)	102.9 (1.4)	61.2 (0.8)	54.3 (0.7)
6.0	0.2265 (55)	96.5 (2.3)	60.0 (1.5)	53.4 (1.3)
6.2	0.1619 (19)	86.4 (1.0)	56.9 (0.7)	50.8 (0.6)
6.4	0.1215 (12)	81.3 (0.8)	55.7 (0.5)	50.0 (0.5)
6.8	0.0730 (12)	76.9 (1.3)	55.7 (0.9)	50.4 (0.8)
∞ Lin.	0	63.6 (2.4)	53.1 (1.6)	48.3 (1.4)
Log.	0	54^{+18}_{-15}	$53.2^{+2.6}_{-7.3}$	$49.1^{+2.3}_{-5.9}$

for which the first-order expansion is exact. The hope is that the nonperturbative (or higher-order perturbative) contributions that are resummed in the effective coupling g_E may compensate high-order terms in the β function which are responsible for the scaling violations. Support for this expectation comes from the observed scaling of ratios of physical quantities (Figs. 4 and 5) within the same β region.

The coefficients c_1 and c_2 have been calculated previously [24], and c_3 has recently been calculated by Allés et al. [25]. The numerical values are:

$$c_1 = (N_C^2 - 1)/(8N_C), \tag{22}$$

$$c_2 = (N_C^2 - 1)[0.020\,427\,7 - 1/(32N_C^2)]/4, \tag{23}$$

$$c_3 = (N_C^2 - 1)N_C(\ 0.006\,659\,9 - 0.020\,411/N_C^2$$
$$+0.034\,339\,9/N_C^4)/6. \tag{24}$$

The plaquette values needed for the conversion into the effective coupling schemes are collected in Table IV. The numbers for $\beta \leq 5.9$ were taken from the collection in Ref. [11]. Starting from the expansion

$$\beta(g) = -\frac{dg}{d\ln a} = -\sum_{n=0}^{\infty} b_n g^{2n+3} \tag{25}$$

of the β function, one rewrites

$$\beta(g_E) = -\frac{dg_E}{d\ln a} = -\frac{dg}{d\ln a}\frac{g}{g_E}\frac{dg_E^2}{dg^2}$$
$$= -b_0 g_E^3 - b_1 g_E^5 - b_2 g_E^7$$
$$+\left\{3b_0\left[2\left(\frac{c_2}{c_1}\right)^2 - \frac{c_3}{c_1}\right] - 2b_1\frac{c_2}{c_1}\right\}g_E^7 + O(g_E^9). \tag{26}$$

The first two terms in this weak-coupling expansion remain unchanged under the substitution. Therefore, an integration again leads to Eq. (18), but with a redefined integration constant

$$\Lambda_E = \Lambda_L \exp\left(\frac{c_2}{2c_1 b_0}\right) \approx 2.075\,6\Lambda_L \quad \text{[for SU(3)]}. \tag{27}$$

This factor is due to a shift of the effective β by a constant in the continuum limit: $g_E^{-2} = g^{-2} - c_2/c_1 + O(g^2)$. In the following we will refer to this scheme as the $\beta_E^{(1)}$

TABLE IV. The average plaquette action $\langle S_\square \rangle$, measured on large lattice volumes. The values for $\beta \leq 5.9$ are taken from the collection in Ref. [11] while the other numbers are our new results, obtained on 32^4 lattices, and one $24^3 \times 32$ lattice ($\beta = 6.2$).

β	$\langle S_\square \rangle$
5.7	0.451 00 (80)
5.8	0.432 36 (5)
5.9	0.418 25 (6)
6.0	0.406 262(17)
6.2	0.386 353 (8)
6.4	0.369 353 (5)
6.8	0.340 782 (5)

scheme. As one can see from Fig.6(a) (open squares) and Table III this kind of (numerical) resummation of the asymptotic series equation (20) leads to considerably reduced logarithmic corrections ($C \approx 2.5$).

As an additional check of this improvement technique we consider in the following an "alternative" effective coupling scheme $\beta_E^{(2)}$. Our idea is to introduce a coupling g_2 by inverting the relation

$$\langle S_\square \rangle = c_1 g_2^2 + c_2 g_2^4. \tag{28}$$

This amounts to truncating the weak coupling expansion equation (20) after the second term.[4] A short calculation yields

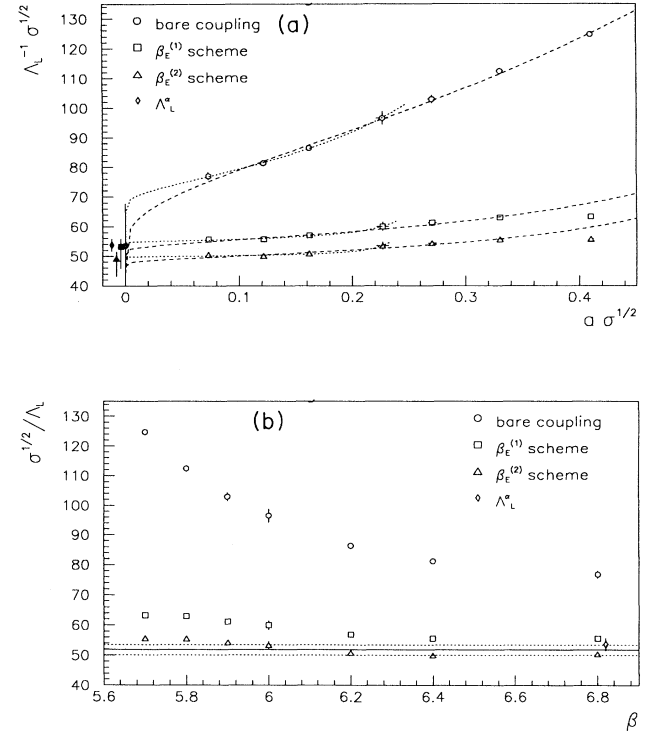$$\beta(g_2) = -b_0 g_2^3 - b_1 g_2^5 - b_2 g_2^7 - 3b_0\frac{c_3}{c_1}g_2^7 + O(g_2^9). \tag{29}$$

FIG. 6. The parameter Λ_L^{-1}, as calculated from Eq. (18), versus (a) the lattice spacing a and (b) the inverse bare coupling β for the different effective coupling schemes. The values for $\beta \leq 5.9$ were obtained by the MT_C Collaboration [23]. In Fig. 6(a) the extrapolated continuum values (solid symbols), and different fit curves are plotted additionally. The solid line in Fig. 6(b) corresponds to $\sqrt{\sigma} = 51.9^{+1.6}_{-1.8}\Lambda_L$.

[4]One can generalize this scheme by truncating in higher orders n. This is of little interest, however (unless one is interested in numerical studies of the impact of a particular higher-loop contribution on the observed scaling violations), since the β function has only been calculated up to $O(g^5)$. Moreover, one would retrieve the bare coupling scheme at n sufficiently large.

Because of $g_2^{-2} = g^{-2} + O(g^2)$ the integration constant Λ_L remains unchanged in respect to the original bare coupling scheme.

If we compare the third-order terms of the two effective schemes [Eqs. (26) and (29)], we find, explicitly,

$$\beta(g) = \beta(g_E(g)) + 5.3 \times 10^{-4} g^7 + O(g^9)$$
$$= \beta(g_2(g)) + 4.02 \times 10^{-3} g^7 + O(g^9). \qquad (30)$$

This means that the correction of the β function through the three-loop contribution is much larger for the $\beta^{(2)}$ than for the $\beta^{(1)}$ scheme.[5] Nevertheless, at least within the investigated β region, the qualitative behavior of both

schemes is the same as can be seen in Fig. 6(a). For the $\beta^{(2)}$ scheme the correction coefficient ($C \approx 0.9$) of the continuum extrapolation equation (19) is even smaller than for the $\beta_E^{(1)}$ scheme. In Fig. 6(a) we have included the estimates for the asymptotic Λ_L^{-1} values (and the Λ_L^{-1} from the running coupling) as solid symbols.

The extrapolated values for both effective schemes are, respectively,

$$\sqrt{\sigma} = 53.2^{+2.6}_{-7.3} \Lambda_L^{(1)} \qquad (31)$$

$$= 49.1^{+2.3}_{-5.9} \Lambda_L^{(2)}. \qquad (32)$$

TABLE V. The potential values $V(\mathbf{R})$ (in lattice units a^{-1}), "corrected" values $V(R)$, and ground-state overlaps $C(\mathbf{R})$ for $\beta = 6.8$, $V = 32^4$.

R	Path	$V(\mathbf{R})$	$V(R)$	$C(\mathbf{R})$
1.00	1	0.3107 (6)	0.3210 (10)	0.950 (3)
1.41	2	0.3855 (11)	0.3794 (12)	0.951 (4)
1.73	4	0.4188 (19)	0.4098 (20)	0.946 (8)
2.00	1	0.4236 (14)	0.4266 (14)	0.929 (5)
2.24	3	0.4428 (13)	0.4397 (14)	0.934 (5)
2.45	5	0.4559 (15)	0.4509 (15)	0.936 (6)
2.83	2	0.4696 (20)	0.4656 (20)	0.923 (8)
3.00	1	0.4725 (14)	0.4709 (14)	0.931 (6)
3.00	6	0.4751 (18)	0.4705 (19)	0.924 (7)
3.46	4	0.4906 (31)	0.4861 (31)	0.923 (12)
4.00	1	0.5000 (18)	0.4970 (19)	0.916 (7)
4.24	2	0.5079 (23)	0.5039 (23)	0.939 (9)
4.47	3	0.5105 (22)	0.5068 (22)	0.916 (9)
4.90	5	0.5178 (28)	0.5139 (28)	0.913 (11)
5.00	1	0.5193 (19)	0.5159 (20)	0.924 (8)
5.20	4	0.5230 (32)	0.5190 (32)	0.929 (13)
5.66	2	0.5312 (29)	0.5273 (30)	0.920 (12)
6.00	1	0.5325 (25)	0.5289 (25)	0.907 (10)
6.00	6	0.5357 (29)	0.5317 (30)	0.918 (12)
6.71	3	0.5421 (27)	0.5383 (27)	0.917 (11)
6.93	4	0.5469 (42)	0.5430 (42)	0.916 (16)
7.00	1	0.5463 (27)	0.5426 (27)	0.921 (11)
7.07	2	0.5474 (36)	0.5436 (37)	0.928 (15)
7.35	5	0.5504 (32)	0.5466 (32)	0.923 (13)
8.00	1	0.5568 (34)	0.5531 (34)	0.910 (13)
8.49	2	0.5623 (44)	0.5584 (44)	0.911 (17)
8.66	4	0.5644 (47)	0.5605 (47)	0.930 (19)
8.94	3	0.5663 (37)	0.5625 (37)	0.911 (15)
9.00	1	0.5671 (36)	0.5633 (36)	0.920 (14)

[5]Note that the difference between the β functions for both effective schemes is independent of c_3 to this order.

TABLE V. *(Continued.)*

R	Path	$V(\mathbf{R})$	$V(\mathbf{R})$	$C(\mathbf{R})$
9.00	6	0.5651 (37)	0.5612 (37)	0.911 (15)
9.80	5	0.5733 (41)	0.5695 (41)	0.908 (16)
9.90	2	0.5745 (48)	0.5707 (48)	0.925 (19)
10.00	1	0.5743 (44)	0.5705 (44)	0.904 (17)
10.39	4	0.5777 (53)	0.5739 (53)	0.905 (21)
11.00	1	0.5830 (49)	0.5792 (49)	0.913 (19)
11.18	3	0.5818 (49)	0.5780 (49)	0.903 (20)
11.31	2	0.5841 (50)	0.5803 (50)	0.898 (20)
12.00	1	0.5887 (55)	0.5849 (55)	0.895 (21)
12.00	6	0.5900 (55)	0.5862 (55)	0.901 (22)
12.12	4	0.5941 (60)	0.5902 (60)	0.928 (24)
12.25	5	0.5918 (53)	0.5879 (53)	0.912 (21)
12.73	2	0.5962 (64)	0.5923 (64)	0.918 (26)
13.00	1	0.5987 (56)	0.5949 (56)	0.912 (22)
13.42	3	0.5998 (61)	0.5960 (61)	0.894 (24)
13.86	4	0.6031 (75)	0.5993 (75)	0.895 (29)
14.00	1	0.6055 (62)	0.6017 (62)	0.899 (24)
14.14	2	0.6052 (73)	0.6014 (73)	0.893 (29)
14.70	5	0.6096 (70)	0.6058 (70)	0.895 (27)
15.00	1	0.6097 (68)	0.6059 (68)	0.895 (27)
15.00	6	0.6102 (69)	0.6064 (69)	0.895 (27)
15.56	2	0.6139 (81)	0.6101 (81)	0.904 (32)
15.59	4	0.6163 (81)	0.6125 (81)	0.910 (32)
15.65	3	0.6144 (73)	0.6106 (73)	0.895 (29)
16.00	1	0.6151 (74)	0.6113 (74)	0.878 (29)
16.97	2	0.6246 (88)	0.6209 (88)	0.886 (34)
17.15	5	0.6248 (78)	0.6210 (78)	0.895 (31)
17.32	4	0.6258 (94)	0.6220 (94)	0.883 (36)
17.89	3	0.6296 (90)	0.6258 (90)	0.880 (35)
18.00	6	0.6312 (88)	0.6274 (88)	0.885 (34)
18.39	2	0.6337 (99)	0.6299 (99)	0.899 (39)
19.05	4	0.6394(109)	0.6357(109)	0.900 (43)
19.60	5	0.6402 (95)	0.6364 (95)	0.874 (36)
19.80	2	0.6440(105)	0.6402(105)	0.882 (41)
20.79	4	0.6486(117)	0.6448(117)	0.875 (44)
21.00	6	0.6496(108)	0.6458(108)	0.879 (42)
21.21	2	0.6526(118)	0.6489(118)	0.891 (46)
22.52	4	0.6610(131)	0.6573(131)	0.889 (51)
22.63	2	0.6545(128)	0.6508(128)	0.847 (48)
24.00	6	0.6688(123)	0.6650(123)	0.863 (47)
24.25	4	0.6694(142)	0.6657(142)	0.862 (53)
25.98	4	0.6791(151)	0.6753(151)	0.866 (57)
27.71	4	0.6908(162)	0.6871(162)	0.848 (60)

We average these numbers, and estimate the error from the combined χ^2 distributions, taking into account the fact that they are correlated. This leads to $\sqrt{\sigma} = 50.8^{+2.4}_{-6.6}\Lambda_L^E$. The result is in nice agreement with the ratio extracted from the running coupling [$\sqrt{\sigma} = 53.7(2.1)\Lambda_L^\alpha$, Eq. (17)]. Using this additional information we obtain

$$\sqrt{\sigma} = 51.9^{+1.6}_{-1.8}\Lambda_L. \tag{33}$$

This result may be converted into any continuum renormalization scheme such as the modified minimal subtraction ($\overline{\text{MS}}$) scheme. By exploiting the relation $\Lambda_{\overline{\text{MS}}} = 28.81\Lambda_L$ [26] we get

$$\frac{\Lambda_{\overline{\text{MS}}}}{\sqrt{\sigma}} = 0.555^{+0.019}_{-0.017}. \tag{34}$$

Let us finally comment that the two approaches presented in this paper for the determination of the QCD scale parameter Λ, namely, to analyze (a) $g^2(\Lambda aR)$ and (b) its inverse $\Lambda a(g^2)$ in terms of the two-loop predictions, Eqs. (13) and (18), are complementary and supportive to each other because higher-order corrections to methods (a) and (b) are anticorrelated. In our running coupling (string tension) analysis we observe the "effective" Λ_L to decrease (increase) with the energy scale. Since the central value of our "upper limit" Λ_L^α is smaller than that of our "lower limit" Λ_L^E we are in the position to state relatively small errors for $\Lambda_{\overline{\text{MS}}}$.

In Fig. 6(b) we have plotted the Λ_L^{-1} data versus β in order to visualize the slow approach of the bare coupling data toward the asymptotic value, and the improvement achieved by the use of *effective* couplings.

IV. DISCUSSION

We have demonstrated that medium-scale computer experiments are able to determine the Λ parameter of SU(3) Yang-Mills theory within a reasonable accuracy (that can compete with QCD experiments). For this result, it has been important to study both infrared and ultraviolet aspects in order to verify the reliability of the

continuum extrapolation. We might say that we have been lucky to get hold of *asymptotia* within our means. This is due to the discovery that the running coupling *constant* is well described within this theory by the two-loop formula down to a scale of about 1 GeV.

If nature continues to be nice to us, and the inclusion of dynamical quarks results only in a β shift of quenched predictions it is possible to predict experimental numbers like $\alpha_S(M_Z)$, as explained in Ref. [2]. Obviously, it is preferable to repeat this study in full QCD on the level of teraflops power. In the meantime, further improvements of lattice techniques are of great interest. A promising route has been proposed by Lüscher et al. [27], and tested on SU(2) Yang-Mills theory. These authors start from a volume-dependent coupling $g(L)$ which allows them to reach large energies on small lattices.

After completion of this work we received a paper by Booth, Michael, and collaborators [28] that contains a running coupling study for SU(3) gauge theory up to $\beta = 6.5$. Their results are fully consistent with ours.

APPENDIX A: POTENTIAL VALUES

In this appendix we are stating the potential values measured on a 32^4 lattice at $\beta = 6.8$. The corresponding numbers for the other β values can be found in Ref. [6]. The on- and off-axis paths are numbered in the following way:

	Path No.					
	1	2	3	4	5	6
Path (X,Y,Z)	$(1,0,0)$	$(1,1,0)$	$(2,1,0)$	$(1,1,1)$	$(2,1,1)$	$(2,2,1)$
Elementary distance M	1	1.41	2.24	1.73	2.45	3

The results for the potential $V(\mathbf{R})$ (in lattice units), as well as for the "corrected" $V(R)$, and the corresponding ground-state overlaps $C(\mathbf{R})$ are collected in Table V. The data is plotted (among the other curves) in Fig. 4.

[1] See, e.g., the review article by T. Hebbeker, Phys. Rep. **217**, 69 (1992).

[2] A.X. El-Khadra, G. Hockney, A.S. Kronfeld, and P.B. Mackenzie, Phys. Rev. Lett. **69**, 729 (1992); P.B. Mackenzie, in *Lattice '91*, Proceedings of the International Symposium, Tsukuba, Japan, 1991, edited by Y. Iwasaki, M. Okawa, and A. Ukawa [Nucl. Phys. B (Proc. Suppl.) **26**, 369 (1992)].

[3] C. Michael, Phys. Lett. B **283**, 103 (1992).

[4] M. Lüscher, R. Sommer, U. Wolff, and P. Weisz, CERN Report No. CERN-TH 6566/92 1992 (unpublished).

[5] UKQCD Collaboration, S.P. Booth, K.C. Bowler, D.S. Henty, R.D. Kenway, B.J. Pendleton, D.G. Richards, A.D. Simpson, A.C. Irving, A. McKerrell, C. Michael, P.W. Stephenson, M. Teper, and K. Decker, Phys. Lett. B **275**, 424 (1992).

[6] G.S. Bali and K. Schilling, Phys. Rev. D **46**, 2636 (1992).

[7] A. Hasenfratz and P. Hasenfratz, Phys. Lett. **93B**, 165 (1980); Nucl. Phys. **B193**, 210 (1981).

[8] G. Parisi, in *High Energy Physics—1980,* Proceedings of the XXth International Conference, Madison, Wisconsin, 1980, edited by L. Durand and L.G. Pondrom, AIP Conf. Proc. No. 68 (AIP, New York, 1981), p. 1531.

[9] Y.M. Makeenko and M.I. Polikarpov, Nucl. Phys. **B205**, 386 (1982).

[10] S. Samuel, O. Martin, and K. Moriarty, Phys. Lett. **152B**, 87 (1984).

[11] J. Fingberg, U. Heller, and F. Karsch, Bielefeld Report No. BI-TP 92-26, 1992 (unpublished).

[12] N. Cabibbo and E. Marinari, Phys. Lett. **119B**, 387 (1982).

[13] S.L. Adler, Phys. Rev. D **23**, 2901 (1981).

[14] A. Kennedy and B. Pendleton, Phys. Lett. **156B**, 393 (1985).

[15] J. Hoek, M. Teper, and J. Waterhouse, Nucl. Phys. **B288**, 589 (1987).

[16] M. Campostrini, A. Di Giacomo, M. Maggiore, H. Panagopoulos, and E. Vicari, Phys. Lett. B **225**, 403 (1989).

[17] APE Collaboration, M. Albanese *et al.*, Phys. Lett. B **192**, 163 (1987).

[18] B. Efron, Ann. Statist. **7**, 1 (1979).

[19] R. Gupta *et al.*, Phys. Rev. D **36**, 2813 (1987).

[20] C.B. Lang and C. Rebbi, Phys. Lett. **115B**, 137 (1982).

[21] M. Lüscher, K. Symanzik, and P. Weisz, Nucl. Phys. **B173**, 365 (1980); M. Lüscher, *ibid.* **B180**, 317 (1981).

[22] A. Billoire, Phys. Lett. **104B**, 472 (1981).

[23] *MT_C* Collaboration, K.D. Born, R. Altmeyer, W. Ibes, E. Laermann, R. Sommer, T.F. Walsh, and P. Zerwas, in *Lattice '90*, Proceedings of the International Symposium, Tallahassee, Florida, 1990, edited by U.M. Heller, A.D. Kennedy, and S. Sanielevici [Nucl. Phys. B (Proc. Suppl.) **20**, 394 (1991)].

[24] A. DiGiacomo and G.C. Rossi, Phys. Lett. **100B**, 481 (1981); A. DiGiacomo and G. Paffati, Phys. Lett. **108B**, 327 (1982); U. Heller and F. Karsch, Nucl. Phys. **B251**, 254 (1985).

[25] B. Allés, M. Campostrini, A. Feo, and H. Panagopoulos, Pisa Report No. IFUP-TH-32192, 1992 (unpublished).

[26] R. Dashen and D.J. Gross, Phys. Rev. D **23**, 2340 (1981).

[27] M. Lüscher, R. Narayanan, P. Weisz, and U. Wolff, Nucl. Phys. **B384**, 168 (1992).

[28] S.P. Booth, D.S. Henty, A. Hulsebos, A.C. Irving, C. Michael, and P.W. Stephenson, Liverpool Report No. LTH 285, 1992 (unpublished).